Development of a Face Hobbed Spiral Bevel Gearset

Hermann J. Stadtfeld

Bevel Gear Technology
Chapter 2, Continued

This article is the fourth installment in *Gear Technology's* series of excerpts from Dr. Hermann J. Stadtfeld's book, *Gleason Bevel Gear Technology*. The first three excerpts can be found in our June, July and August 2015 issues.

In the previous chapter, we demonstrated the development of a face-milled spiral bevel gearset. In this section, an analogue face-hobbed bevel gearset is derived.

— **Hermann J. Stadtfeld**

For this example the following data are given:

Method	continuous indexing with Gleason face hobbing	
Tooth depth along face width	parallel	
Shaft angle	Σ	90°
Offset	a = TTX	0 mm
Number of pinion teeth	z_1	13
Number of ring gear teeth	z_2	35
Outer ring gear pitch diameter	D_{02}	190 mm
Face width	$b_1 = b_2$	30 mm
Mean spiral angle	$\beta_1 = \beta_2$	30°
Pinion hand of spiral	$HOSP_1$	left-hand
Nominal cutter radius	R_w	88 mm
Number of cutter starts	Z_w	17
Pressure angle	$\alpha_C = \alpha_D$	20°
Profile shift factor	$x = x_1 = -x_2$	0
Tooth depth factor	f_{Depth}	1
Top-root-clearance factor	f_{CL}	0.2
Profile side shift factor	$x_S = x_{S1} = -x_{S2}$	0
Pinion addendum	h_{K1}	$(f_{Depth} + x) * m_n = 1.0 m_n$
Pinion dedendum	h_{F1}	$(f_{Depth} + f_{CL} - x) * m_n = 1.2 m_n$
Ring gear addendum	h_{K2}	$(f_{Depth} - x) * m_n = 1.0 m_n$
Ring gear dedendum	h_{F2}	$(f_{Depth} + f_{CL} + x) * m_n = 1.2 m_n$

Wanted are the design data of the pinion and ring gear blanks as well as the cutter specifications and the basic machine settings.

Calculation of Blank Data

Since the subject of this section is, as in the previous section ("Gear Mathematics for Bevel & Hypoid Gears," *Gear Technology*'s August 2015 issue), a spiral bevel gearset with parallel depth teeth and the same dimensions and tooth numbers, the blank dimensions in both cases are also identical. Tables 1 and 2 repeat the actual design data for the blanks of pinion and ring gear.

Table 1	Numerical ring gear blank specifications		
Ring Gear - Blank Data			
Variable	**Explanation**	**Value**	**Dimension**
z_2	number of ring gear teeth	35	-
$RINR_2$	inner cone distance (along root line)	69.56	mm
$RAUR_2$	outer cone distance (along root line)	99.56	mm
$GATR_2 = \gamma_2$	pitch angle	69.62	°
$GAKR_2$	face angle	69.62	°
$GAFR_2$	root angle	69.62	°
$ZTKR_2$	pitch apex to crossing point	0.00	mm
$ZKKR_2$	face apex to crossing point	−4.27	mm
$ZFKR_2$	root apex to crossing point	5.12	mm
$DOMR_2 = m_{f2}$	face module	4.63	mm
HGER	whole depth of teeth	8.80	mm

Table 2	Numerical pinion blank specifications		
Pinion - Blank Data			
Variable	Explanation	Value	Dimension
z_1	number of teeth pinion	13	-
$RINR_1$	inner cone distance (along root line)	58.42	mm
$RAUR_1$	outer cone distance (along root line)	88.42	mm
$GATR_1 = \gamma_1$	pitch angle	20.38	°
$GAKR_1$	face angle	20.38	°
$GAFR_1$	root angle	20.38	°
$ZTKR_1$	pitch apex to crossing point	0.00	mm
$ZKKR_1$	face apex to crossing point	−11.49	mm
$ZFKR_1$	root apex to crossing point	13.78	mm
$DOMR_1 = mf_1$	face module	4.63	mm
HGER	whole depth of teeth	8.80	mm

Calculation of the Cutter Head Geometry

It must first be mentioned that based on the continuous indexing, the relative cutting velocity of the blades is not oriented tangentially to the circumference of the cutter. Figure 1 shows a triangular vector graphic. While R_{Wi-1} rotated counter-clockwise, the cutter roll circle rolls on a base circle. The tip of the cutter head vector moves therefore not from "A" to "B", but from "A" to "C". The relation between roll circle and base circle is equal to the relation of the number of cutter head blade groups to

the number of generating gear teeth. The addition of the base circle radius and the radius of the roll circle amounts to the radial distance Krumme (Ref. 4) applied an unrolling of the arcs in order to determine the angle δ_W which is enclosed by the current cutter radius and the dashed drawn epicycloid. Here the infinitesimal observation shown at the top of Figure 1 is proposed, which confirms the result from Krumme. Subsequently, the blade offset angle can be calculated as follows:

$$\delta_W = asin\,\{(d\varphi * R_M * \cos \text{ß} * Z_W/Z_E)\,/\,(d\varphi * R_W)\} \tag{1}$$

After canceling of $d\varphi$ and the substitution:

$$R_M * \cos \text{ß} / Z_E = m_n/2 \tag{2}$$

The result is the following formula:

$$\delta_W = asin\{(m_n * Z_W)\,/\,(2 * R_W)\} = 22.73° \tag{3}$$

Figure 1   The continuous working cutter head.

This angle δ_W describes the precise relations of the relative cutting velocity direction for the applied nominal cutter radius between cutter blades and the plane generating gear. The relationships between cutter blades and real generating gears and real work gears will differ slightly from the calculated relative velocity direction δ_W. However, the value δ_W is well-suited for first estimations and for the design of cutter heads.

Based on the continuous indexing motion, not only an epicyclic flank form but also a spiral angle — which is increased by δ_W — is created. It now becomes interesting to introduce the blade offset angle δ_W in order to control the orientation of the technological blade angles similar to the single indexing method. The blade offset angle is used to calculate the corresponding blade offset values *XSME* (Fig. 1).

The nominal cutter radius of 88 mm was chosen about equal to the mean cone distance R_M. This seems to be a good choice for a bevel gearset manufactured in face hobbing, since the effective curvature radius of the epicycloid at the mean cone distance turns out smaller than the cutter radius. Although the nominal cutter radius is already given, the effective radii for the inside and outside blades of ring gear and pinion cutter must be calculated according to the chosen cutting method. Since the chosen method is Gleason TRI-AC, which uses equally the cutter circumference spaced inside and outside blades without profile shift ($x = 0$), the following graphics and calculations are applicable (Fig. 2).

Figure 2 shows the pinion cutter head (top) and the ring gear cutter head (bottom). The generating plane intersects the blades at the height of the calculation point. The generation of the correct tooth thickness (except the backlash) happens in case of equally spaced blades automatically. The blade tips protrude about their respective dedendum height (h_F) beyond the generating plane. This makes the blade contours in Figure 2 not exactly congruent, but by the backlash values different on the flanks and by the clearance values differ-
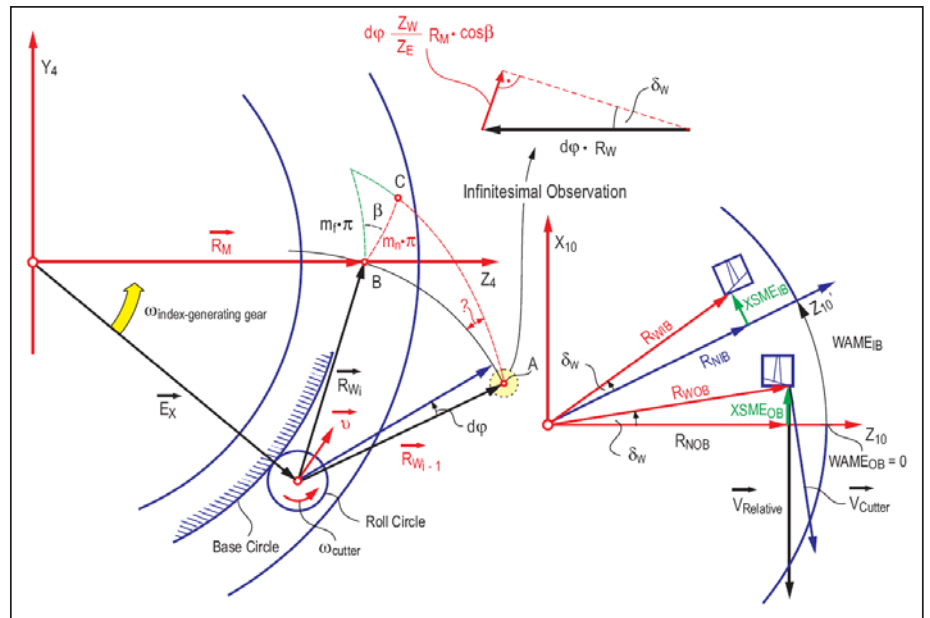
ent at the roots. Just like in the previous section, as now with this second flank generating example, a conjugate mating pair should be achieved. For this purpose the backlash is set to zero for this calculation.

The following calculations are used to determine the required cutter head and blade parameters:

$$ALFW_1 = ALFW_2 = ALFW_3 = ALFW_4 = \alpha = 20.00° \tag{4}$$

The blade offset angle δ_W is depending on the individual gear design and is calculated as:

$$\delta_W = arcsin((Z_W * m_n)\,/\,(2 * R_W)) = 22.73° \tag{5}$$

The normal radius R_N of the cutter head is the adjacent side to the angle δ_W in a rectangular triangle with R_W as hypotenuse:
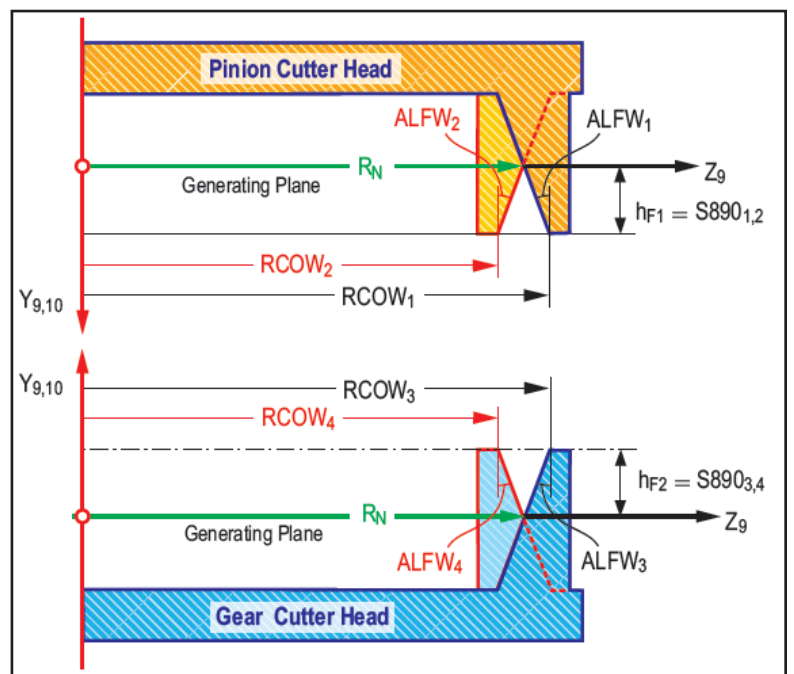

Figure 2   Pinion and ring gear cutter geometry.

$$R_N = R_W \cdot \cos \delta_W = 81.17 \, \text{mm} \tag{6}$$

The calculation of the normal blade point radii is calculated (Fig. 2) (the module and the h_F values are equal to those in the previous section in the August 2015 issue):

$$RCOW_1 = R_N - SPLF/4 + h_{F1} \cdot \tan ALFW_1 = 82.92 \, \text{mm} \tag{7}$$

$$RCOW_2 = R_N + SPLF/4 - h_{F1} \cdot \tan ALFW_2 = 79.42 \, \text{mm} \tag{8}$$

$$RCOW_3 = R_N - SPLF/4 + h_{F2} \cdot \tan ALFW_3 = 82.92 \, \text{mm} \tag{9}$$

$$RCOW_4 = R_N + SPLF/4 - h_{F2} \cdot \tan ALFW_4 = 79.42 \, \text{mm} \tag{10}$$

The blade height above the face of the cutter head (distance from coordinate system 9 to blade tip) amounts to:

$$S890_1 = S890_2 = h_{F1} = 4.80 \, \text{mm} \tag{11}$$

$$S890_3 = S890_4 = h_{F2} = 4.80 \, \text{mm} \tag{12}$$

The blade offset is the opposite side of the angle δ_W in a rectangular triangle with R_W as hypotenuse:

$$XSME_1 = XSME_2 = +R_W \cdot \sin \delta_W = 34.00 \, \text{mm} \tag{13}$$

$$XSME_3 = XSME_4 = -R_W \cdot \sin \delta_W = -34.00 \, \text{mm} \tag{14}$$

The blade following angles *WAME* around the cutter head axis (Fig. 1) in case of equal blade spacing amount to:

$$WAME_1 = 180° / Z_W = 10.59° \tag{15}$$

$$WAME_2 = 0.00° \tag{16}$$

$$WAME_3 = -180° / Z_W = -10.59° \tag{17}$$

$$WAME_4 = 0.00° \tag{18}$$

All parameters printed in bold are required for the definition of the pinion and ring gear cutter heads. Those results are summarized in Table 3.

Calculation of Basic Settings for the Cutting Machine

The cutter head center in Figure 3 is placed in a position in order to generate the same spiral angle of 30°, which cannot be found in the extension of the flank line normal but along a straight line that is rotated clockwise about δ_W. The calculation of the basic settings for the present example are shown below. Those calculations are identical to the calculations in the previous section (August 2015 issue), *excepting the newly introduced angle* δ_W. The solution vector in this observation is the eccentricity vector E_X, which already contains several of the wanted machine settings.

The triangular vector of the ring gear generation:

$$\vec{E_X} = \vec{R_M} - \vec{R_W} \tag{19}$$

with:

$$\vec{R_M} = \{0., 0., R_M\} = \{0., 0., 86.34\} \tag{20}$$

$$\vec{R_W} = \{-R_W \cos(\beta - \delta_W), 0., R_W \sin(\beta - \delta_W)\} = \{-87.29, 0., 11.14\} \tag{21}$$

$$\text{resulting in: } \vec{E_X} = \{87.29, 0., 75.20\} \tag{22}$$

The following machine settings can be obtained from the E_X vector:

$$\text{Center roll position: } W450_{3,4} = \arctan(E_{XX}/E_{XZ}) = 49.27° \tag{23}$$

$$\text{Radial distance: } TZMM_{3,4} = \sqrt{E_{XX}^2 + E_{XZ}^2} = 115.22 \, \text{mm} \tag{24}$$

$$\text{Sliding base: } TYMM_{3,4} = E_{XY} = 0.00 \, \text{mm} \tag{25}$$

Additional machine settings can be found from the graphical relationship in Figure 3:

$$\text{Machine root angle: } AWIM_{3,4} = -90° - \gamma_2 = -159.62° \tag{26}$$

$$\text{Machine csenter to crossing point: } TZ2M_{3,4} = 0.00 \, \text{mm} \tag{27}$$

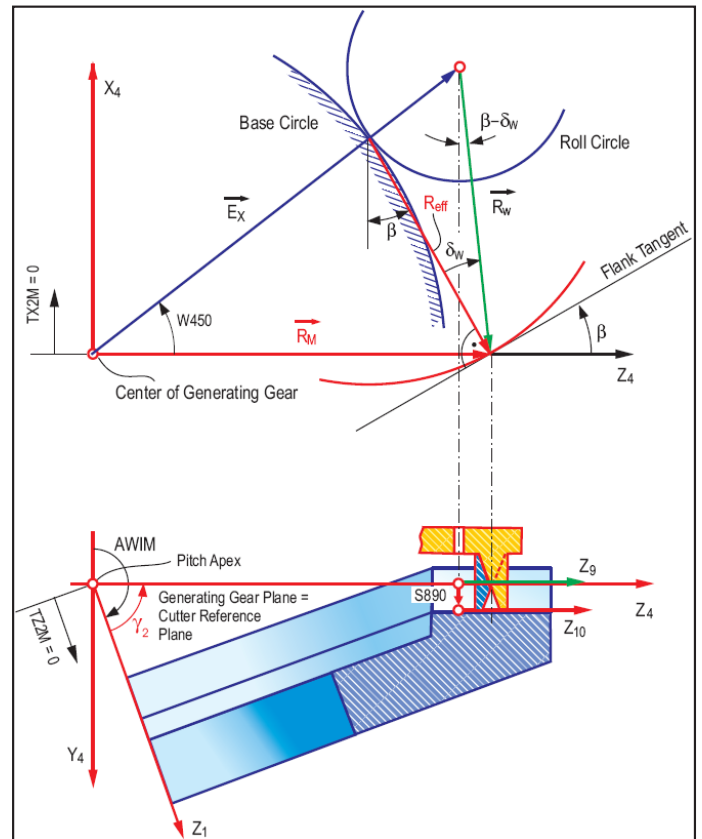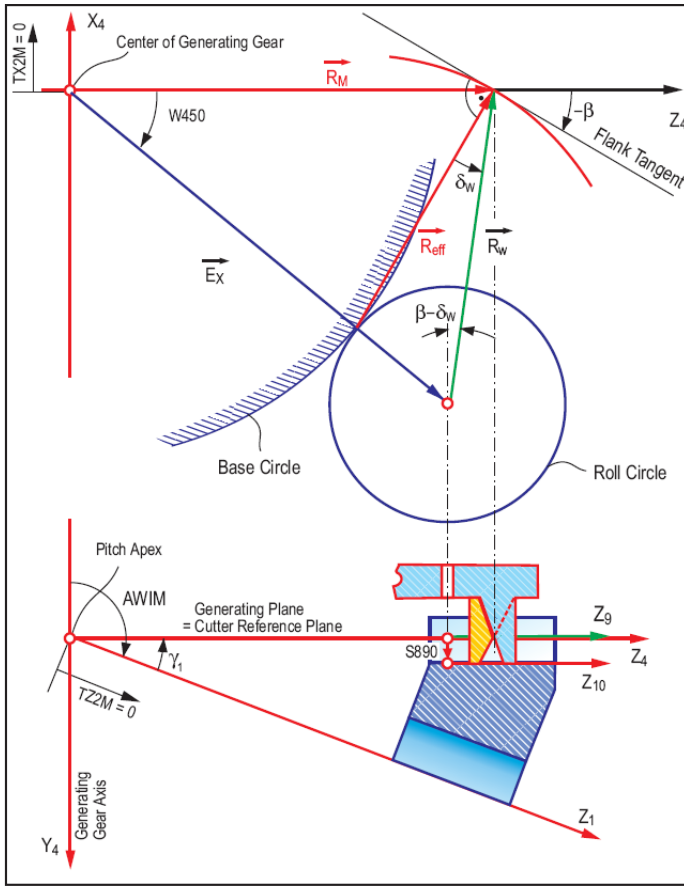**Figure 3   Ring gear, basic machine model, upper graphic: → front view; lower graphic → top view.**

Table 3	Cutter head and blade specifications		
Cutter Head and Blade Data			
Variable	Explanation	Value	Dimension
$S890_{1,2}$	reference point to blade tip pinion	4.80	mm
$S890_{3,4}$	reference point to blade tip gear	4.80	mm
$WAME_1$	blade phase angle pinion convex	10.59	°
$WAME_2$	blade phase angle pinion concave	0.00	°
$WAME_3$	blade phase angle ring gear convex	−10.59	°
$WAME_4$	blade phase angle ring gear concave	0.00	°
$XSME_{1,2}$	blade offset in pinion cutter head	34.00	mm
$XSME_{3,4}$	blade offset in ring gear cutter head	−34.00	mm
$RCOW_1$	cutter point radius pinion inside blade	82.92	mm
$RCOW_2$	cutter point radius pinion outside blade	79.42	mm
$RCOW_3$	cutter point radius ring gear inside blade	82.92	mm
$RCOW_4$	cutter point radius ring gear outside blade	79.42	mm
$ALFW_1$	blade angle pinion inside blade	20.00	°
$ALFW_2$	blade angle pinion outside blade	20.00	°
$ALFW_3$	blade angle ring gear inside blade	20.00	°
$ALFW_4$	blade angle ring gear outside blade	20.00	°

[www.geartechnology.com]

Figure 4 Pinion, basic machine model, upper graphic: → front view, lower graphic → top view.

Offset in the machine: $TX2M_{3,4} = 0.00\,\text{mm}$ (28)

Further values such as cutter head tilt $WXMM_{3,4}$ and tilt orientation $WYMM_{3,4}$ are also zero in the observed conjugate design.

For the exact definition of the ring gear to be generated, the ratio of roll between generating gear and work gear as well as the indexing ratio between cutter head and work gear are still missing. From Equations 11 and 12 in Chapter 1 ("Basics of Gear Theory, Part 2," July 2015 *Gear Technology*) the ratio can be computed with:

$$UDIF_{3,4} = \sin\gamma_2 = 0.937425$$ (29)

The ratio of roll number requires at least a mantissa with 6 digits, since the influence onto the gear geometry is correspondingly sensitive. The indexing ratio is the number of work gear teeth divided by the number of cutter starts:

$$UTEI_{3,4} = Z_2 / Z_W = 2.058824$$ (30)

For the value of the indexing ratio, the input of at least 5 digits behind the decimal point is recommended.

The triangular vector of the pinion generation: (31)

$$\text{With: } \vec{R_W} = \{R_W \cos(\beta - \delta_W), 0., R_W \sin(\beta - \delta_W)\} = \{87.29, 0., 11.14\}$$ (32)

$$\text{Resulting in: } \vec{E_x} = \{-87.29, 0., 75.20\}$$

The following machine settings can be obtained from the E_x vector:

Table 4 Geometrical and kinematical machine settings

Variable	Explanation	Value	Dimension
Machine Basic Settings			
$WXMM_{1,2}$	cutter head tilt pinion	0.00	°
$WXMM_{3,4}$	cutter head tilt ring gear	0.00	°
$WYMM_{1,2}$	swivel angle pinion	0.00	°
$WYMM_{3,4}$	swivel angle ring gear	0.00	°
$W450_{1,2}$	center roll position pinion	−49.26	°
$W450_{3,4}$	center roll position ring gear	−49.26	°
$TYMM_{1,2}$	sliding base position pinion	0.00	mm
$TYMM_{3,4}$	sliding base position ring gear	0.00	mm
$TZMM_{1,2}$	radial distance pinion	115.22	mm
$TZMM34$	radial distance ring gear	115.22	mm
$AWIM_{1,2}$	machine root angle pinion	−110.38	°
$AWIM_{3,4}$	machine root angle ring gear	−159.62	°
$TX2M_{1,2}$	pinion offset in the machine	0.00	mm
$TX2M_{3,4}$	ring gear offset in the machine	0.00	mm
$TZ2M_{1,2}$	machine center to crossing point pinion	0.00	mm
$TZ2M_{3,4}$	machine center to crossing point gear	0.00	mm
$UTEI_{1,2}$	indexing ratio of pinion cutting	0.764706	-
$UTEI_{3,4}$	indexing ratio of ring gear cutting	2.058824	-
$UDIF_{1,2}$	ratio of roll for pinion cutting	0.348187	-
$UDIF_{3,4}$	ratio of roll for ring gear cutting	0.937425	-

Center of roll: $W450_{1,2} = \arctan(E_{XX} / E_{XZ}) = -49.26°$ (33)

Radial distance: $TZMM_{1,2} = \sqrt{E_{XX}^2 + E_{XZ}^2} = 115.22\,\text{mm}$ (34)

Sliding base: $TYMM_{1,2} = E_{XY} = 0.00\,\text{mm}$ (35)

Additional machine settings can be found from the graphical relationship in Figure 4:

Machine root angle: $AWIM_{1,2} = -90° - \gamma_1 = -110.38°$ (36)

Machine center to crossing point: $TZ2M_{1,2} = 0.00\,\text{mm}$ (37)

Offset in the machine: $TX2M_{1,2} = 0.00\,\text{mm}$ (38)

Further values, such as cutter tilt $WXMM_{1,2}$ and tilt orientation $WYMM_{1,2}$ are also zero in the observed conjugate design. For the exact definition of the pinion to be generated, the ratio of roll between generating gear and work gear during the roll is still missing. From Equations 11 and 12 in Chapter 1 ("Basics of Gear Theory, Part 2," July 2015 *Gear Technology*) the ratio can be computed with:

$$UDIF_{1,2} = \sin\gamma_1 = 0.348187$$ (39)

$$UTEI_{1,2} = Z_1 / Z_W = 0.764706$$ (40)

All bold-printed values calculated in this section are input values for a bevel gear cutting simulation program whose functionality was discussed in the previous section (August 2015 issue). The machine settings of this section are summarizesd in Table 4.

Simulation of the Gear Cutting Process and Tooth Contact Analysis of the Face Hobbed Spiral Bevel Gearset Example

For the tooth contact analysis results of the gearset generated in a continuous cutting process, (face hobbing) applies basically the same as explained for the face milled example in the previous section (August 2015 issue). The Ease-Offs for coast

and drive side are perfectly con- jugate, the motion graphs are zero and the contact lines extend over the entire active flank area (Fig. 5). Also, in case of the face hobbed example, large unused stripes can be observed towards the root of the pinion. The expla- nations given in the previous sec- tion apply here as well; a posi- tive profile shift $X_1 = 0.5$ would be sufficient to achieve a better and more effective profile contact ratio. ◉

Figure 5   Graphical results of roll simulation (TCA) of a face hobbed gear pair.

References

1. Stadtfeld, H.J. *Handbook of Bevel and Hypoid Gears - Calculation, Manufacturing and Optimization,* Rochester Institute of Technology, Rochester, NY, March 1993.
2. Stadtfeld, H.J. "The Ultimate Motion Graph," *Journal of Mechanical Design,* Vol. 122, September 2000.
3. Weck, M., B. Neupert, H. Schriefer and H.J. Stadtfeld. "Das Lauf- und Beanspruchungsverhalten bogenverzahnter Kegelradgetriebe," *Reports of the 21st to 28th Annual Conference Gear and Transmission Research,* 1980 to 1987, WZL-RWTH Aachen.
4. Krumme, W. *Klingelnberg Spiralkegelraeder, Berechnung, Herstellung und Einbau,* Springer Publishing, Berlin/Heidelberg/New York, 1967.
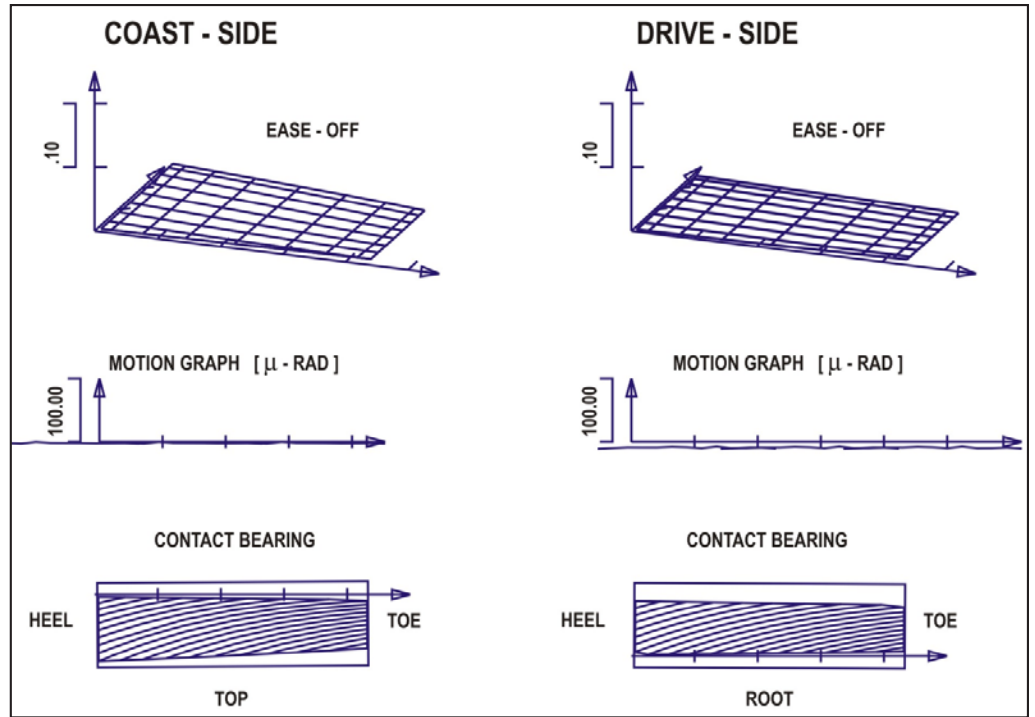5. Wildhaber, E. "Skew Hypoid Gears," *American Machinist,* 1946.
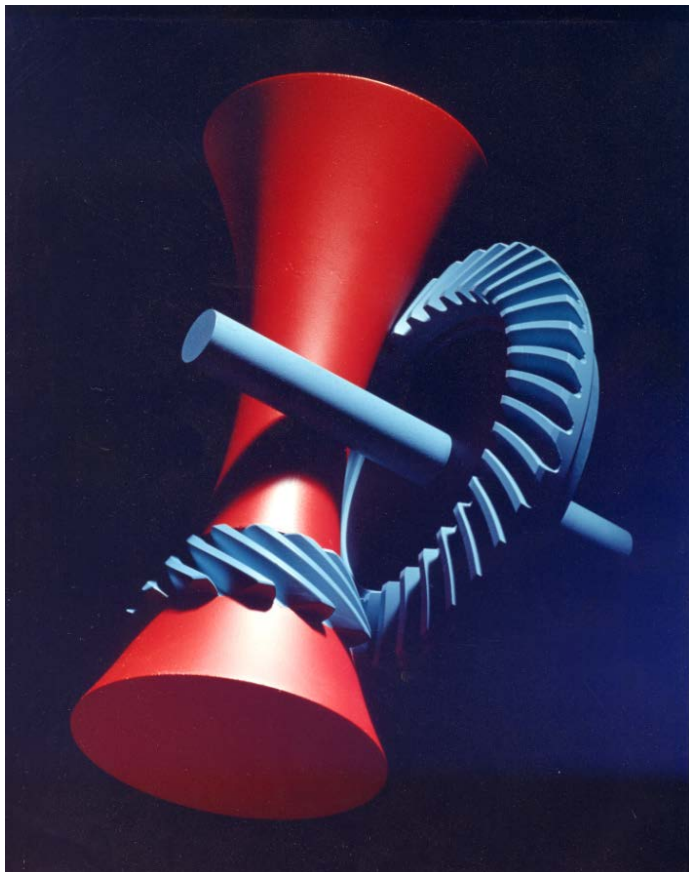
Figure 6   Hyperbolic pitch element of a gearset with hypoid offset (hypoid gears).

Dr. Hermann J. Stadtfeld received in 1978 his B.S. and in 1982 his M.S. degrees in mechanical engineering at the Technical University in Aachen, Germany; upon receiving his Doctorate, he remained as a research scientist at the University's Machine Tool Laboratory. In 1987, he accepted the position of head of engineering and R&D of the Bevel Gear Machine Tool Division of Oerlikon Buehrle AG in Zurich and, in 1992, returned to academia as visiting professor at the Rochester Institute of Technology. Dr. Stadtfeld returned to the commercial workplace in 1994 — joining The Gleason Works — also in Rochester — first as director of R&D, and, in 1996, as vice president R&D. During a three-year hiatus (2002–2005) from Gleason, he established a gear research company in Germany while simultaneously accepting a professorship to teach gear technology courses at the University of Ilmenau. Stadtfeld subsequently returned to the Gleason Corporation in 2005, where he currently holds the position of vice president, bevel gear technology and R&D. A prolific author (and frequent contributor to Gear Technology), Dr. Stadtfeld has published more than 200 technical papers and 10 books on bevel gear technology; he also controls more than 50 international patents on gear design, gear process, tools and machinery.